11-15-2023

Back-Imaging of Pressure-Sensitive Paint to Determine Close Proximity Ground Effects of Propellers

Jacob Kulig
University of Dayton, kuligj1@udayton.edu

Back-Imaging of Pressure-Sensitive Paint to Determine Close Proximity Ground Effects of Propellers

Honors Thesis

Jacob Kulig

Department: Mechanical Engineering

Advisor: Carson Running, Ph.D.

November 2023

Back-Imaging of Pressure-Sensitive Paint to Determine Close Proximity Ground Effects of Propellers

Honors Thesis

Jacob Kulig

Department: Mechanical Engineering

Advisor: Carson Running, Ph.D.

November 2023

Abstract

The ground effects of propellers have been extensively studied. Although the flow field between a propeller and a ground plate has been theoretically and experimentally analyzed through a variety of methods, there are limitations to the current work, especially in globally analyzing the nature of the flow along the ground plate and unsteady analysis. This study provides a proof of concept that back-imaged pressure-sensitive paint (PSP) can successfully analyze the pressure along such a ground plate. The pressure field was successfully measured utilizing this technique. By analyzing the pressure field in the frequency domain, the unsteady characteristics of the flow were able to be quantitatively determined, further revealing the separation between tangential and radial flow seen in previous work. This provides a promising area for potential use of PSP to more fully understand the flow field under rotor blades in ground effect, thereby improving safety and performance.

Acknowledgements

The author would like to thank the entire University of Dayton Low Speed Wind Tunnel Lab, Sidaard Gunasekaran's lab group and Dr. Carson Running's lab group for their support, advice, and equipment throughout this project. He would especially like to thank Jacky Cai and Dr. Gunasekaran for their input and assistance with the background and implications of this work in regards to rotorcraft and their previous work.

University *of* Dayton

Table of Contents

Nomenclature

AA-PSP	=	Anodized Aluminum Pressure Sensitive Paint
CFD	=	Computational Fluid Dynamics
I	=	Intensity (of PSP emission)
N	=	Frame
p	=	Pressure
p'	=	Fluctuating Component of Pressure
$\bar{p}$	=	Mean Pressure
PC-PSP	=	Polymer-Ceramic Pressure Sensitive Paint
PSP	=	Pressure Sensitive Paint
sf	=	spatial filtering parameter
tf	=	temporal filtering parameter

Sub/superscripts

kul	=	denotes quantity measured by descrete pressure transducers (Kulites)
PSP	=	denotes quantity measured by PSP
ref	=	denotes reference quantity

1 Introduction

Ground effect on small propellers, where an impermeable planar surface parallel and in close proximity to the rotor, has been studied theoretically ([1, 2, 3]) and experimentally ([2, 3, 4, 5, 6, 7]) for decades. The ground plate offers two benefits to the rotor: an increase in thrust produced, and a decrease in power required, for a given rotational speed, which combine into propulsive efficiency augmentation [8]. Other than the benefit of propeller performance, a complicated flow field has also been observed on the ground plate when placing the rotor in close proximity to the ground, including a center tangential flow and an outer radial flow regime [8, 9]. With the emerging use of quadcopters and applications of air taxis, studies on rotor and propeller ground effect have garnered

more attention in recent years [8, 9, 10, 11, 12]. Ground effect on multi-rotor aerial vehicles brings additional complicity to the flow field where additional fountain flow and recirculation fountain flow are observed when placing the rotor within two diameters from each other in hover [10]. Understanding the flow field on the ground-plate benefits the operation of the modern air taxi takeoff and landing as the rotor outwash in the ground effect creates safety concerns for humans near the landing zone [13]. Avoiding the area where fountain flow and strong radial flow occur would ensure the safe operation of the multi-rotor drone and air-taxi vehicles.

Visualizing and measuring this flow field's interaction at the ground has been completed through several methods. Dekker et al. [10] utilized coulometric velocimetry to study the flow field around rotors in ground effect scenarios, allowing a visualization of this flow field. Cai et al. [9], meanwhile, qualitatively analyzed the flow field at the ground plate using three techniques: tufts that reveal flow direction and strengths, smoke visualization, and titanium dioxide oil on the ground surface. These techniques allow various aspects of the flow to be visualized. By combining this intuition with discrete pressure transducer (Kulite) data, global quantitative measurements of pressure in various conditions could be deduced [9]. However, this method is inherently limited by the need to correlate discrete pressure measurements to the global flow field. Although these techniques remain extremely useful, this limits their ability to fully understand the flow and thereby improve the safety and performance of rotorcraft. To capture unsteady phenomenon or provide a direct, quantitative analysis of the entire flow field at the ground interaction, a global measurement technique is required.

Pressure-sensitive paint (PSP) represents a potential method to fill this requirement. PSP is a pressure sensor applied to a model's surface. The paint contains a luminophore chemical that responds to the partial pressure of oxygen. When illuminated by a specific wavelength of light, this luminophore emits at a different wavelength. The intensity of this emission is inversely related to the partial pressure of oxygen. Using a camera, the intensity of the PSP can be recorded at each pixel in an image. Knowing the relationship between pressure and this intensity, the pressure at each pixel in the image can therefore

be calculated. This provides a global pressure field over the test object [14, 15]. This method is often utilized in wind tunnel testing and as verification for computational fluid dynamics (CFD) models [14]. In this experiment, PSP is applied to the ground surface under a propeller. This theoretically allows the pressure at each location to be calculated over time, which is very useful information for analyzing this situation.

Fast PSP is a subset of PSP designed for unsteady aerodynamics. Traditional PSP can be relatively slow to respond to changes in pressure relative to other techniques, such as discrete sensors. Fast PSP is altered to allow the oxygen to more easily interact with the luminophore in the paint, reducing the response time (and increasing the frequency response). This allows the paint to quickly react to changes in the pressure field, allowing unsteady aerodynamic phenomenon to be captured [15]. There are two main types of fast PSP: anodized aluminum (AA-PSP) and polymer-ceramic (PC-PSP). AA-PSP uses a porous, anodized aluminum model that increases the surface area and aids bonding of the luminophore [15]. PC-PSP includes small particles of ceramic, either mixed with the paint or applied before the luminophore. This also increases the surface area and porosity of the paint, allowing oxygen to reach the luminophore with less difficulty and decrease the response time [15]. In this study, PC-PSP is utilized to help capture potential unsteady effects.

PSP relies on the surface of the model being in sight of the camera during data collection. The propeller, however, partially blocks the surface of the ground from being viewed during ground effect testing; this led the researchers to investigate back imaging of PSP. In this modification of traditional PSP, the luminophore mixture is applied to a clear substrate. This material is then illuminated and/or imaged from the opposite side of the material, allowing PSP to be utilized without visual access to the surface of the test object [16]. This technique has been attempted and research suggests back imaging and illuminating PSP produces equivalent results to traditional imaging [16]. However, it is still relatively novel. In this study, back-imaging and back-illumination is utilized as the most effective way to avoid visual interference from the propeller.

2 Experimental Setup

The experimental setup is shown in Figure 1. The propeller is attached to a frame on one side of a ground plate. The ground plate is coated with PSP on the side of the propeller (right in the figure, Side B). On the opposing side the laser is utilized to illuminate the PSP while the high speed camera records images (Side A). Images of the physical setup are shown in Figures 2 and 3

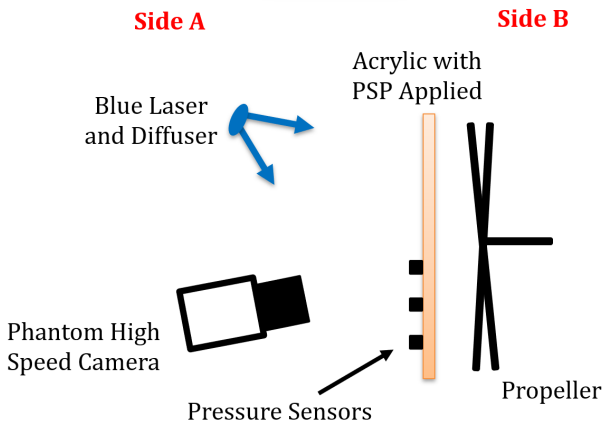

Figure 1: Schematic showing PSP and rotor blade-ground effect setup.

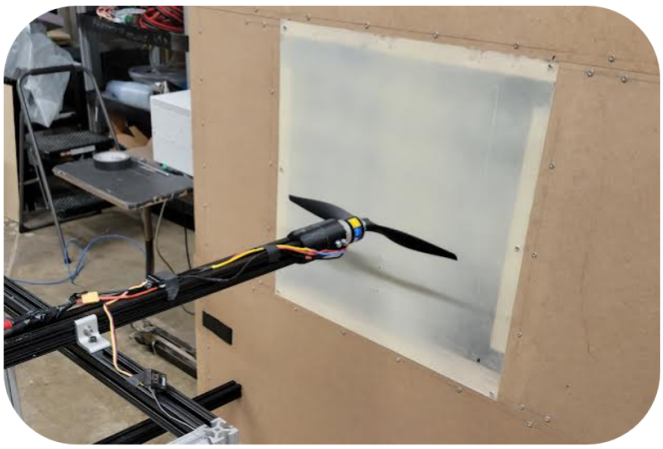

Figure 2: Image of the propeller side of the experimental setup (corresponding to the right side of Figure 1).

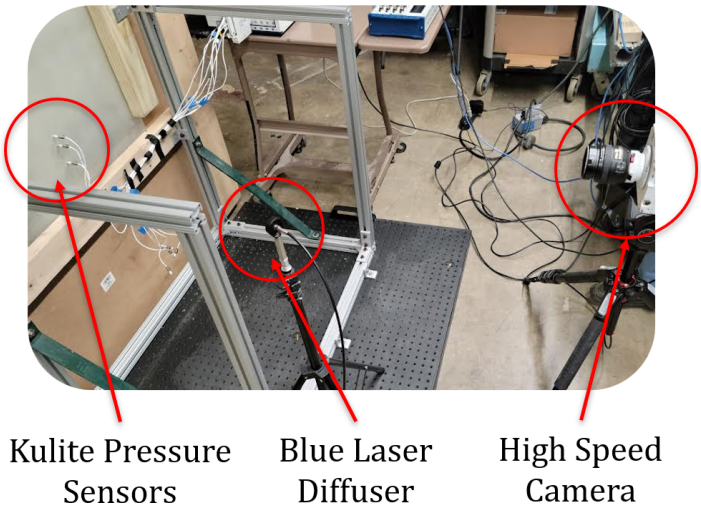

Figure 3: Annotated image of the ”back” side of the experimental setup (the side the PSP is illuminated and imaged from, corresponding to the left side of Figure 1).

2.1 Propeller

The propeller utilized in this experiment is an APC 17 x 7 ”thin electric” propeller [17]. It is rotated by an E-Flight Power 60-400 kV brushless outrunner electric motor and PSW 30-108 constant-voltage power supply. The propeller is kept at a constant 1.7 inches from the ground plate.

2.2 PSP

The PSP utilized is a recipe derived from Sakaue [18]. The ingredients and concentrations are shown in Table 1.

Table 1: Composition of PC-PSP utilized, derived from Sakaue [18]; the total amount is scaled as needed.

Ingredient	Concentration	Function
Ru(ddp)	0.1 mM	Luminophore
RTV rubber	2 g	Binder
Silica particles	3 g	Ceramic Particle
Dichloromethane	50 ml	Solvent

The PSP was mixed thoroughly utilizing a stirring plate and ultrasonic water bath. The mixture was then applied to an acrylic sheet, cleaned with acetone, via a 3M spray gun. The paint was applied in two coats, separated by approximately five minutes.

Based on analysis on aluminum test samples, it is estimated that the paint is 25 to 35 μm thick.

The PSP is illuminated by a Necsel^{TM} Blue DE Laser, with a power of 10 W and typical output at 445 nm. The laser is diffused before reaching the paint with a Thorlabs diffuser. The camera utilized to image the PSP is a Phantom camera recording at 1000 frames per second. Pressure data is simultaneously recorded by the three Kulite pressure sensors, time synchronized with the high speed camera through LabVIEW software.

3 Data Reduction Methodology

The data processing utilizes a combination of techniques from [14, 15, 18, 19, 20]. The process is summarized in the flowchart shown in Figure 4.

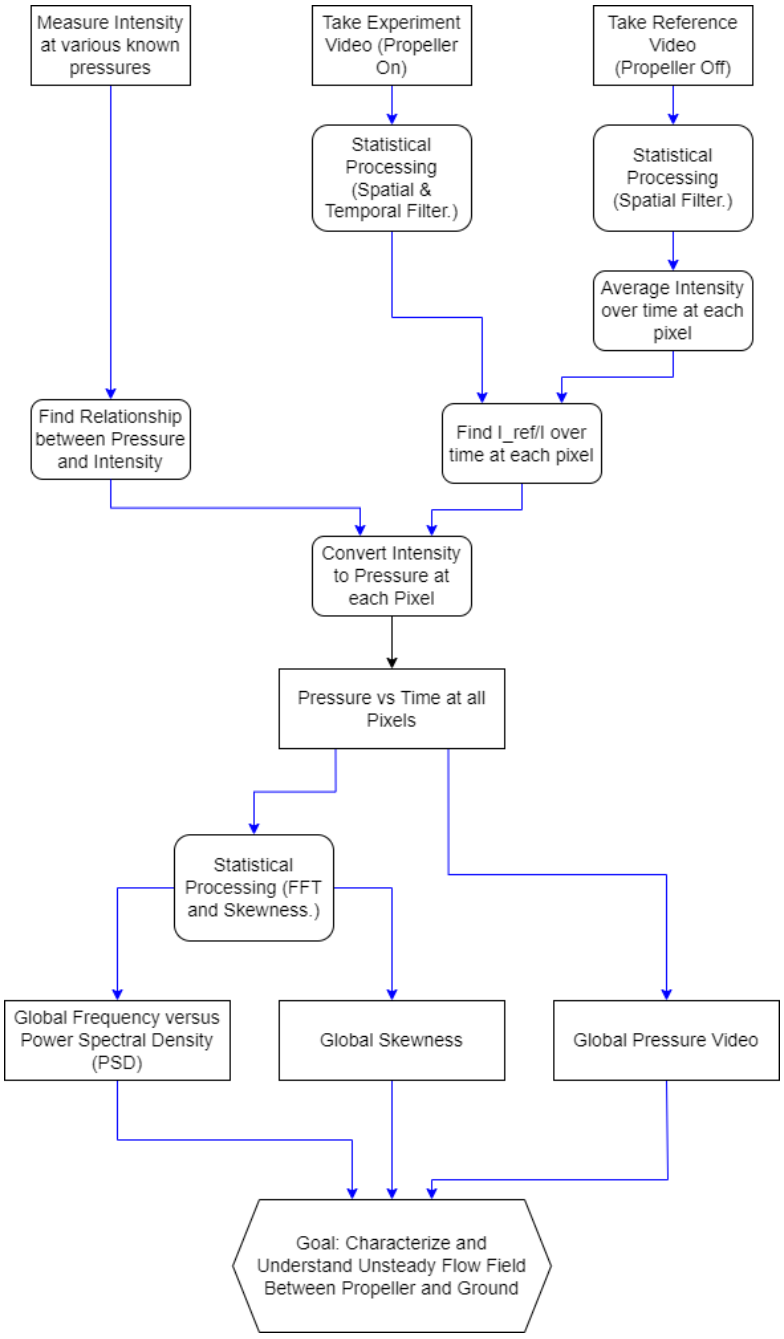

Figure 4: Flowchart showing PC-PSP data processing method utilized in this study, based on [14, 15, 18, 19, 20]

3.1 Data Acquisition

Data was collected simultaneously from the Phantom camera and three Kulite pressure transducers. The Intensity I was recorded at each pixel by the Phantom camera, producing an array of data 960 by 1280 by the number of frames, N. The Kulites, after calibration, provided the gauge pressure P_{kul} at their individual locations. Both data sets were time synchronized with Labview software during the collection process.

3.2 PSP Calculations

This study converts the intensity of the PSP at each individual pixel to pressure utilizing the Stern-Volmer relation, show in Equation 1 [14],

$$\frac{I_{ref}}{I} = A + B\frac{p}{p_{ref}} \quad , \tag{1}$$

where I_{ref} is the reference intensity of the PSP, I is the experimental intensity, p_{ref} and p are the reference and experimental pressures, and A and B are calibration constants. This equation normalizes intensity and pressure, then correlates the two quantities with a inverse linear relationship, where A and B are found through experimental calibration. This method is well established in the use of PSP for its ability to reduce errors due to paint thickness, the camera's viewpoint, and illumination intensity [14, 15]. Interested readers are directed to the work of Gregory et al. [15]. and the book by Liu et al. [14] for more details.

3.2.1 PSP Calibration

In order to utilize the Stern-Volmer relation, the constants A, B, and I_{ref} need to be found. I_{ref} is found by recording the intensity emitted by the PSP in a "propeller off" situation. Assuming this condition is p_{ref}, zero gauge pressure, this provides a matrix 960x1280 in size that can be utilized to normalize the PSP intensity data and remove inconsistencies in the experimental setup illumination, viewing, or paint application.

The constants A and B are found experimentally utilizing an a-priori calibration.

The viewing window of a thermal vacuum chamber is coated in the PSP mixture. At a constant, room temperature, this PSP is exposed to a series of pressures below and at atmospheric pressure and viewed through the window, mimicking the back-imaging experimental setup. One pair of pressure/intensity measurements is then selected as a "reference". $\frac{I_{ref}}{I}$ and $\frac{p}{p_{ref}}$ is calculated for each pressure tested. By applying a linear fit, the calibration constant A, or slope of the linear fit, is found. The calibration constant B is based on the "propeller-off" condition of each test.

3.2.2 Surface Pressure

The pressure p_{psp} is then found at each pixel utilizing these constants and solving the Stern-Volmer relation, producing a matrix 960 by 1280 by N number of frames. This pressure is then spacial filtered to reduce noise in the data by averaging the nearest 11x11 pixels at each frame; no time filtering is applied. The experimental pressure result is then split into a steady and fluctuating component, as shown in Equation 2 [20],

$$p_{PSP} = \bar{p}_{PSP} + p'_{PSP} \quad , \tag{2}$$

where p_{PSP} is the gauge pressure calculated from the PSP at each pixel, $\bar{p}_{PSP}$ is the average pressure at each pixel over time, and p'_{PSP} is the fluctuating component of the pressure. By utilizing $\bar{p}_{PSP}$ and p'_{PSP} separately, unsteady aspects of the flow are more easily observed. This is similar to analysis performed by Running [20] to analyze other unsteady flows.

3.2.3 Power Spectra

To analyze the unsteady nature of the flow under the rotor blade, the Fast Fourier Transform (FFT) is taken of $\frac{p'}{\bar{p}}$ at each point in the PSP pressure data. This provides the power spectral density (PSD) intensity versus frequency, revealing the strength of the unsteady flow at various frequencies in the flow field at each point. This data is displayed as either the maximum PSD intensity or the frequency at which this maximum occurs. It can be displayed in an contour (image showing value at each point) or profile (line showing

quantitative value along a specified axis). This is again similar to analysis performed by Running [20] to analyze other unsteady flows.

In addition, the skewness of the flow was taken at each point. Skewness is a mathematical quantity that reveals to what extent a signal deviates from a Gaussian normal distribution; the value can vary from positive to negative one [20, 21]. This statistic is often utilized in hypersonic shock wave analysis [20]. In the case of PSP for rotor blade ground effect, it has the potential to reveal where in the ground plate the pressure deviates from the average most, providing another measurement of the unsteadiness of the flow. Similar to the PSD intensity and frequency, this information is displayed as contours and associated profiles.

3.3 Blade Interference

As seen in Figure 1, the camera is viewing toward the rotating blade. It can be reasonably questioned whether this blade, by reflecting either the illumination or emission wavelength of the PSP, interfered with the intensity data recorded at each pixel as the blade passed over a given section of the PSP.

To examine this possibility, the pressure recorded by the third Kulite from the center of the propeller (see Figure 1) and the pressure recorded by the PSP immediately above, left, and right of the Kulite, p_{PSP}, were compared over 50 frames. The result is shown in Figure 5. As seen qualitatively in the figure, the data is extremely noisy, even with a spatial filter applied. However, there is a repeating cycle of high and low pressures that matches the Kulite pressure probe data (shown in green). There is an offset in time between them, likely due to a synchronization error between the camera and Kulite data. In addition, there is an offset in recorded pressure. This is likely due to degradation of the paint. Over time, the PSP reduces in emission intensity. As shown in Equation 1, if I decreases, the recorded pressure of the paint increases. However, this is unlikely to affect the frequency results. This gives confidence that the PSP is responding as expected.

If the propeller was affecting the results, however, it would be expected that the

magnitude of the change in the PSP would be significantly different than that of the Kulite. In the figure, this is the case. However, the data is also extremely noisy, and therefore leaves propeller visibility inconclusive.

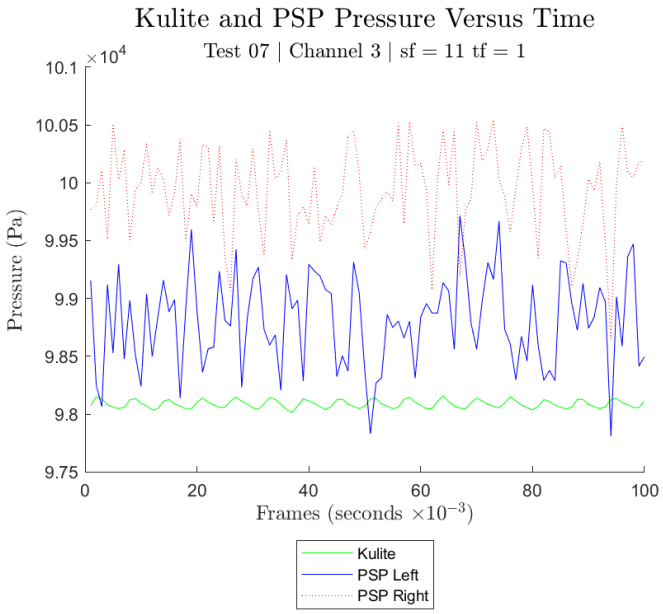

Figure 5: Pressure recorded by PSP left and right of Kulite pressure sensor and pressure recorded by Kulite pressure sensor

The Fast Fourier Transform (FFT) of the PSP near the Kulite provides further evidence about whether the propeller is visible to the camera, potentially interfering with results. Figure 6 shows the FFT Power-Spectral Density (PSD) amplitude horizontally across the ground plate through the center of the propeller. As seen in the figure, the intensity gradually increases across the radius of the propeller. If the propeller was influencing the results, a sharp increase and decrease in PSD intensity would be expected at the inner and outer edges of the propeller blades. This is not seen in this figure.

These results suggest that the PSP intensity measurements are not influenced by the propeller being visually seen by the camera and are in strong correlation with the Kulite measurements. This gives high confidence that the data recorded by the PSP is a valid representation of the pressure field and can be used to characterize the flow field.

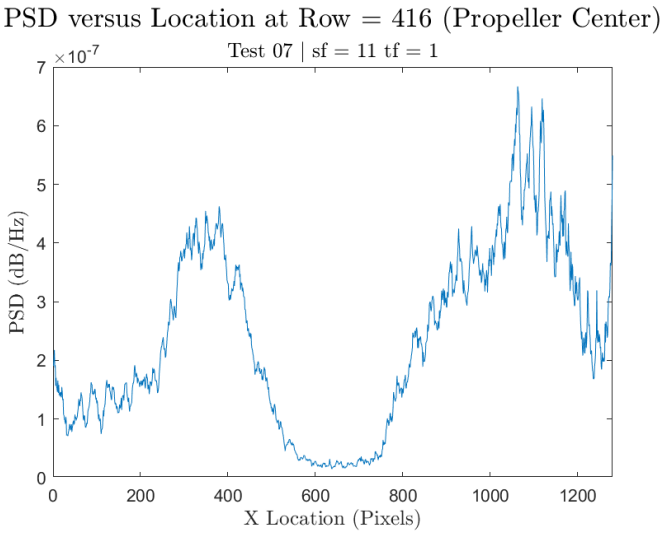

Figure 6: Profile of PSD intensity of $\frac{P'_{PSP}}{\bar{p}_{PSP}}$ over the test plate

4 Results and Discussion

The first result is the instantaneous pressure from the PSP compared to the results of the Kulite, shown in Figure 5. This reveals that the pressure field fluctuates approximately once every five to ten frames.

In addition, the FFT of $\frac{P'_{PSP}}{\bar{p}_{PSP}}$ of a 10x10 pixel segment to the left of the Kulite furthest from the propeller center was compared to the an FFT of $\frac{P'_{kul}}{\bar{p}_{kul}}$. The result is shown in Figure 7. As seen in the graph, the Kulite and PSP show responses at nearly identical frequencies. This suggests, in conjunction with the instantaneous pressure data, that the PSP is successfully recording the pressure field and also responding fast enough to record the unsteady pressure fluctuations.

This result is augmented by the FFT of the PSP-produced pressure field. The contour of the maximum PSD intensity is shown in Figure 8. An associated profile, taken as a line of pixels horizontally along the center of the propeller, quantitatively shows these results in Figure 6. This reveals that the peak unsteady phenomenon forms a ring at between one half and one times the radius of the propeller, and is relatively symmetrical.

This information is augmented by the information shown in Figures 9 and 10. This shows that the frequency of the unsteady phenomenon across the plate is extremely consistent, with deviation only at the center of the propeller and the extreme corners

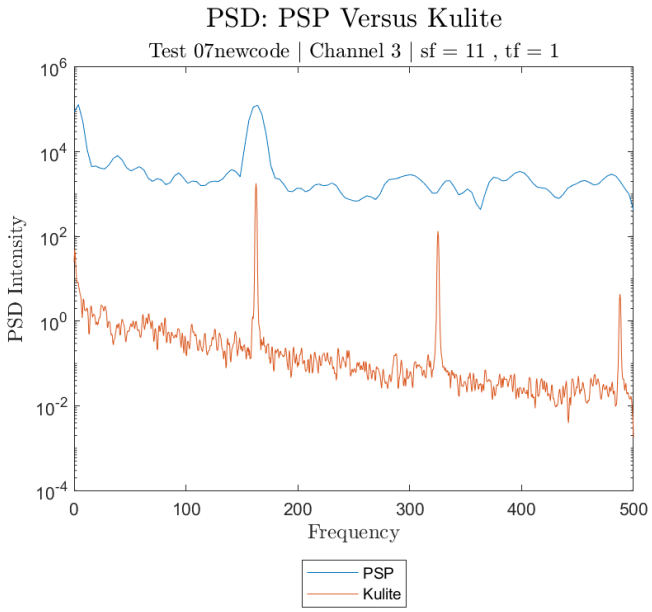

Figure 7: Comparsion of FFT of $\frac{P'_{PSP}}{\bar{p}_{PSP}}$ near Kulite furthest from the propeller center and $\frac{P'_{kul}}{\bar{p}_{kul}}$ of the same Kulite.

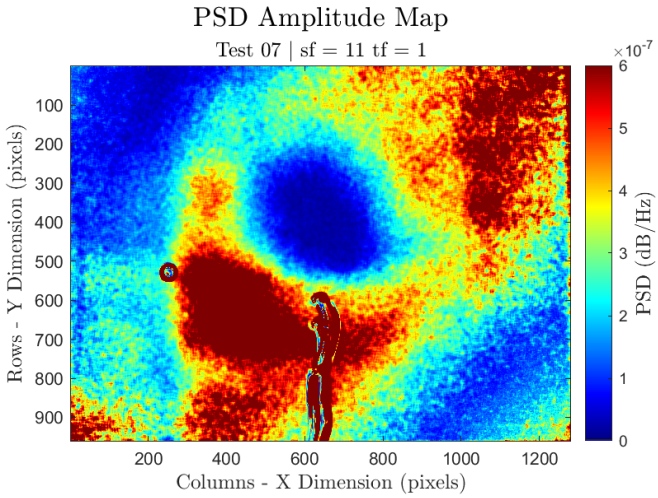

Figure 8: Contour of PSD intensity of P'_{PSP} over the plate.

of the ground plate. This frequency is very close to two times the estimated rotational speed of the propeller, based on its performance in previous testing. The multiplication of two is due to the presence of two blades, causing two pressure fluctuations for each rotation.

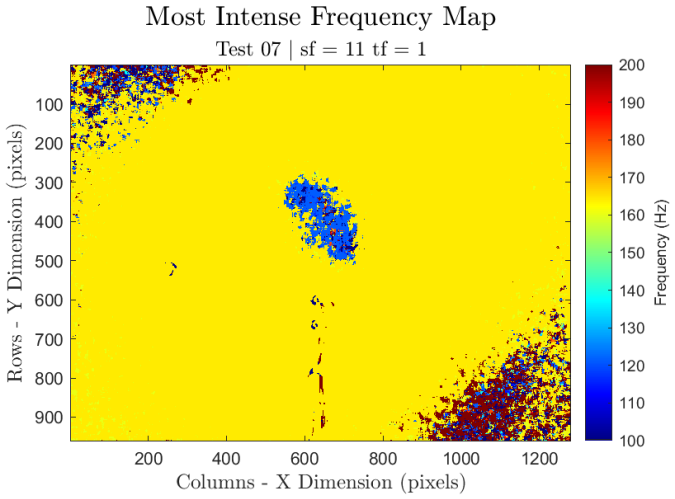

Figure 9: Contour of the frequency at which the max PSD intensity of $\frac{P'_{PSP}}{\bar{p}_{PSP}}$ occurs over the test plate.

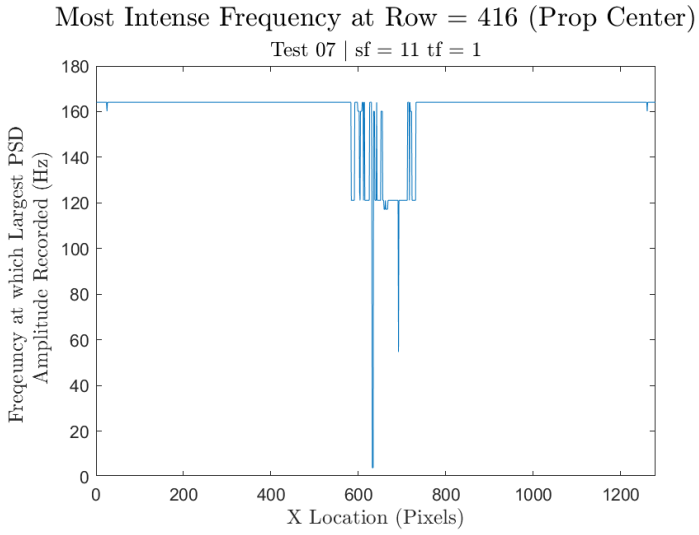

Figure 10: Profile along propeller horizontal centerline (row = 416) of frequency where maximum PSD intensity of $\frac{P'_{PSP}}{\bar{p}_{PSP}}$ occurs.

Finally, the skewness of the pressure was calculated. Again, this result is shown globally in Figure 11 and as a profile in Figure 12. This also shows the beginnings of a ring shape of negative skewness values. This suggests that the locations where the

pressure fluctuates most from the mean is within this area.

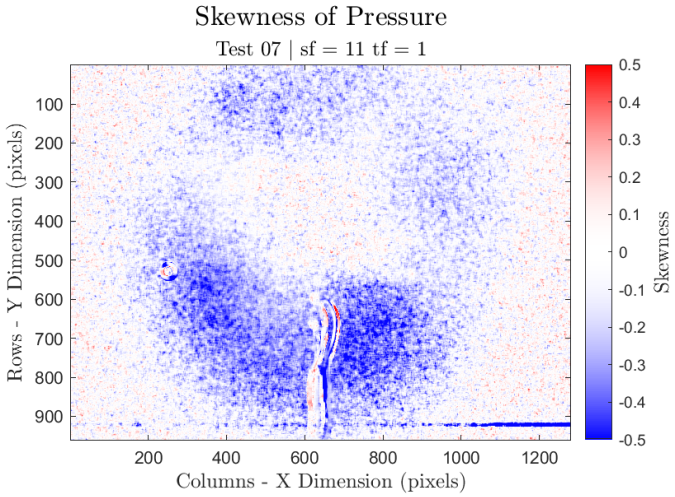

Figure 11: Contour of the skewness of $\frac{P'_{PSP}}{\bar{p}_{PSP}}$

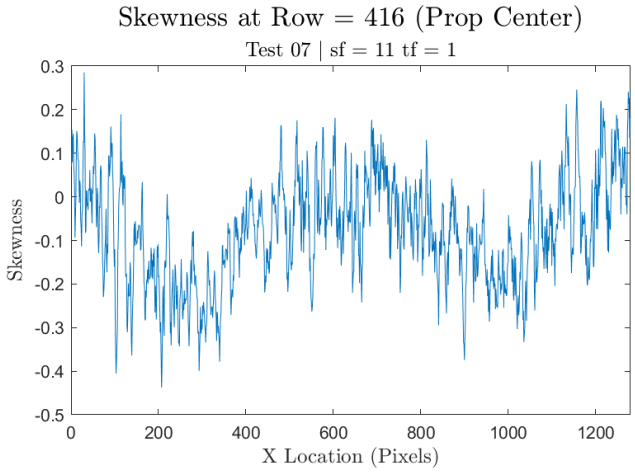

Figure 12: Profile of the the skewness of P'_{PSP} along the horizontal centerline of the propeller.

This information suggests that the strongest unsteady flow occurs in a ring between one half and one times the radius of the propeller from the center of the propeller. This correlates with the qualitative results of Cai et al. [9], who found a stagnation line separating tangential, swirling flow and radial flow at approximately one half the radius of the propeller. These quantitative measurements show that the pressure fluctuation in this region is much stronger than any other location at the ground.

5 Future Work

In additional testing, several points should be investigated further. First, the noise in the data needs to be reduced. The pressure fluctuations being captured (on the order of 100 Pa magnitude) are relatively small compared to the fluctuation of the PSP reading. This could be corrected by more aggressive spatial and temporal filtering of the data or additional layers of noise reduction not yet tried in post processing. Second, future work should match the conditions of previous work by Cai et al. [9]. Finally, more information should be collected on the visibility of the propeller to the camera and its potential influence on results. Although the unsteady analysis shown in Figure 10 suggests that the effect is minimal, it would be far more convincing to see improved agreement in pressure variation magnitude versus time when comparing the Kulite pressure sensors to the PSP in the vicinity of the sensor (see Figure 5).

6 Conclusions

This study utilized back-imaged pressure sensitive paint (PSP) to analyze the pressure field under a small propeller, as would be utilized in unmanned aerial vehicles or small rotorcraft. The PSP was able to successfully image the pressure field and provide global, unsteady analysis of the flow. Is specifically shows that the greatest unsteady phenomenon occurs in a ring shape between approximately one-half radius and one radius of the propeller. This aligns with the division between tangential and radial flow seen qualitatively in previous work [9]. These results show promise in the use of PSP to quantitatively analyze the flow field under small rotorcraft blades in future work.

References

[1] A. Betz. *The Ground Effect on Lifting Propellers*. Tech. rep. 836. NACA, 1937.

[2] Daniel A. Griffiths, Shreyas Ananthan, and J. Gordon Leishman. “Predictions of Rotor Performance in Ground Effect Using a Free-Vortex Wake Model”. In: *Journal of the American Helicopter Society* 50.4 (May 2023), pp. 302–314.

[3] C. Cheeseman and W.E. Bennett. *The effect of the Ground on a Helicopter Rotor in Forward Flight*. Tech. rep. 3021. British R M, 1957.

[4] J. Zbrozek. *Ground Effect on the Lifting Rotor*. Tech. rep. 2347. British R M, 1947.

[5] E.A. Fradenburgh. “The Helicopter as a Ground Effect Machine”. In: *Journal of the American Helicopter Society* (1960), pp. 24–33.

[6] M. Knight and R.A. Hefner. *Analysis of Ground Effect on the Lifting Airscrew*. Tech. rep. TN-835. NACA, 1941.

[7] S. Hayden J. *Effect of the ground on helicopter hovering power required.* Proceedings of the AHS 32nd Forum. 1976.

[8] Gunasekaran S. Ahmed A. Cai J. and V. OL M. “Propeller Ground and Ceiling Effect Parametric Data”. In: *AIAA Journal of Aircraft* 58.3 (Oct. 2020), pp. 700–703. DOI: 10.2514/1.C035839.

[9] Gunasekaran S. Cai J. and V. OL M. “Effect of Partial Ground and Partial Ceiling on Propeller Performance”. In: *AIAA Journal of Aircraft* (Dec. 2022). DOI: 10.2514/1.C036974.

[10] Ragni D. Barrs J. Scarano F. Dekker H. and M. Tuinstra. “Aerodynamic Interactions of Side-by-Side Rotors in Ground Proximity”. In: *AIAA Journal* 60.7 (2022). DOI: 10.2514/1.J061105.

[11] Leang K. He X. *A New Quasi-Steady In-Ground Effect Model for Rotorcraft Unmanned Aerial Vehicles*. ASME 2019 Dynamic Systems and Control Conference, DSCC 2019-9025. 2019. DOI: 10.1115/DSCC2019-9025.

[12] Martin V. Heredia G. Sanchez-Cuevas P. and A. Ollero. *Aerodynamic Effects in Multirotors Flying close to Obstacles: Modelling and Mapping*. Fourth Iberian Robotics conference, pp. 63-74. 2020. DOI: 10.1007/978-3-030-35990-4_6.

[13] M. Calvert and Y. Wenren. *Rotorcraft Outwash and Human Stability*. AIAA Scitech 2019, San Diego, CA, Jan 2019, AIAA 2019-1095. 2019.

[14] Tianshu Liu et al. "Pressure and temperature sensitive paints". In: 2nd. ewerbestrasse 11, 6330 Cham, Swizterland: Springer, 2021.

[15] James W. Gregory et al. "Fast Pressure-Sensitive Paint for Flow and Acoustic Diagnostics". In: *Annual Review of Fluid Mechanics* 46.1 (Sept. 2014), pp. 303–330. DOI: 10.1146/annurev-fluid-010313-141304.

[16] Aaron M Turpin et al. "Back-imaging of polymer-ceramic pressure-sensitive paint". In: *Measurement Science and Technology* 32.10 (Oct. 2021), p. 104008. DOI: 10.1088/1361-6501/ac0a0f.

[17] *APC Propellers | Quality Propellers that are Competition Proven*. URL: https://www.apcprop.com/.

[18] Hirotaka Sakaue, Takuma Kakisako, and Hitoshi Ishikawa. "Characterization and Optimization of Polymer-Ceramic Pressure-Sensitive Paint by Controlling Polymer Content". In: *Sensors* 11.7 (July 2011), pp. 6967–6977. DOI: 10.3390/s110706967.

[19] H. Zare-Behtash et al. "Pressure sensitive paint measurements at high Mach numbers". In: *Flow Measurement and Instrumentation* 52 (Dec. 2016), pp. 10–16. DOI: 10.1016/j.flowmeasinst.2016.02.004.

[20] Carson L. Running and Thomas J. Juliano. "Global measurements of hypersonic shock-wave/bounday-layer interactions with pressure-sensitive paint". In: *Experiments in Fluids* 62.5 (2021), p. 91.

[21] J. S. Bendat and A. G. Piersol. "Random Data: Analysis and Measurement Procedures". In: 4th ed. New York: Wiley, 2010.